2624–2637 *Nucleic Acids Research, 2011, Vol. 39, No. 7* *Published online 7 December 2010*
doi:10.1093/nar/gkq1245

Molecular anatomy of the *Streptococcus pyogenes* pSM19035 partition and segrosome complexes

Nora E. Soberón, Virginia S. Lioy, Florencia Pratto, Andrea Volante and Juan C. Alonso*

Departamento de Biotecnología Microbiana, Centro Nacional de Biotecnología, CSIC, 28049 Madrid, Spain

Received May 12, 2010; Revised November 16, 2010; Accepted November 17, 2010

ABSTRACT

Vancomycin or erythromycin resistance and the stability determinants, δω and ωεζ, of Enterococci and Streptococci plasmids are genetically linked. To unravel the mechanisms that promoted the stable persistence of resistance determinants, the early stages of *Streptococcus pyogenes* pSM19035 partitioning were biochemically dissected. First, the homodimeric centromere-binding protein, ω_2, bound *parS* DNA to form a short-lived partition complex 1 (PC1). The interaction of PC1 with homodimeric δ [δ_2 even in the apo form (Apo-δ_2)], significantly stimulated the formation of a long-lived ω_2·*parS* complex (PC2) without spreading into neighbouring DNA sequences. In the ATP·Mg^{2+} bound form, δ_2 bound DNA, without sequence specificity, to form a transient dynamic complex (DC). Second, *parS* bound ω_2 interacted with and promoted δ_2 redistribution to co-localize with the PC2, leading to transient segrosome complex (SC, *parS*·ω_2·δ_2) formation. Third, δ_2, in the SC, interacted with a second SC and promoted formation of a bridging complex (BC). Finally, increasing ω_2 concentrations stimulated the ATPase activity of δ_2 and the BC was disassembled. We propose that PC, DC, SC and BC formation were dynamic processes and that the molar ω_2:δ_2 ratio and *parS* DNA control their temporal and spatial assembly during partition of pSM19035 before cell division.

INTRODUCTION

Accurate distribution of a newly replicated genome to daughter cells at cell division is a precise process, however this process is prone to occasional error. Low-copy number plasmids of the Inc18 family such as pSM19035, make use of at least two active stabilization systems, partition and toxin–antitoxin (TA), rather than relying on random segregation of plasmid monomers (1–3). pSM19035 encodes three loci (Rep, Par and TA) whose expression is regulated by the homodimeric centromere binding protein (CBP) ω_2 [(4), Figure 1A]. The toxin of the TA locus, which consists of two *trans*-acting proteins (the ε_2 antitoxin and ζ toxin), inhibits the growth of cells that lose the plasmid (1,2). The Rep locus comprises a small antisense RNA and homodimeric CopS ($CopS_2$), both involved in regulation of plasmid copy number, and the RepS protein which activates replication [(4), Figure 1A]. The *par* locus consists of two sets of three *cis*-acting *parS* centromeres and two homodimeric *trans*-acting proteins, δ_2 (ParA-like) and ω_2 (ParB-like), which allow the plasmid to be actively segregated to daughter cells [(1,2), Figure 1A and B]. Given the genetic linkage between the stability determinants δ–ω and ω–ε–ζ and erythromycin and/or vancomycin resistance in Enterococci and Streptococci (5), the characterization of both loci is relevant to understanding the persistence of resistance determinants in Firmicutes. To understand how plasmids are segregated, we have studied the early stages of the pSM19035 partition mechanism.

The partition machinery of low-copy number plasmids and bacterial chromosomes is of two main types: type I (ParAB) and type II (ParMR) (6–9). The majority of plasmids and bacterial chromosomes carry a partition locus of the ParAB type. ParAB systems are further subdivided into those whose ParA has an N-terminal extension needed for autoregulated expression (type Ia) and those whose proteins, in addition to lacking the ParA extension, are relatively small (type Ib) (6–9). Several GFP-fusion derivatives of ParA have been localized in the cell (6–8). In the absence of their cognate ParB, each

*To whom correspondence should be addressed. Tel: +3491585 4546; Fax: +3491585 4506; Email: jcalonso@cnb.csic.es
Present address:
Florencia Pratto, Genetics and Biochemistry Branch, NIDDK, National Institutes of Health, Bethesda, MD 20892, USA.

The authors wish it to be known that, in their opinion, the first two authors should be regarded as joint First Authors.

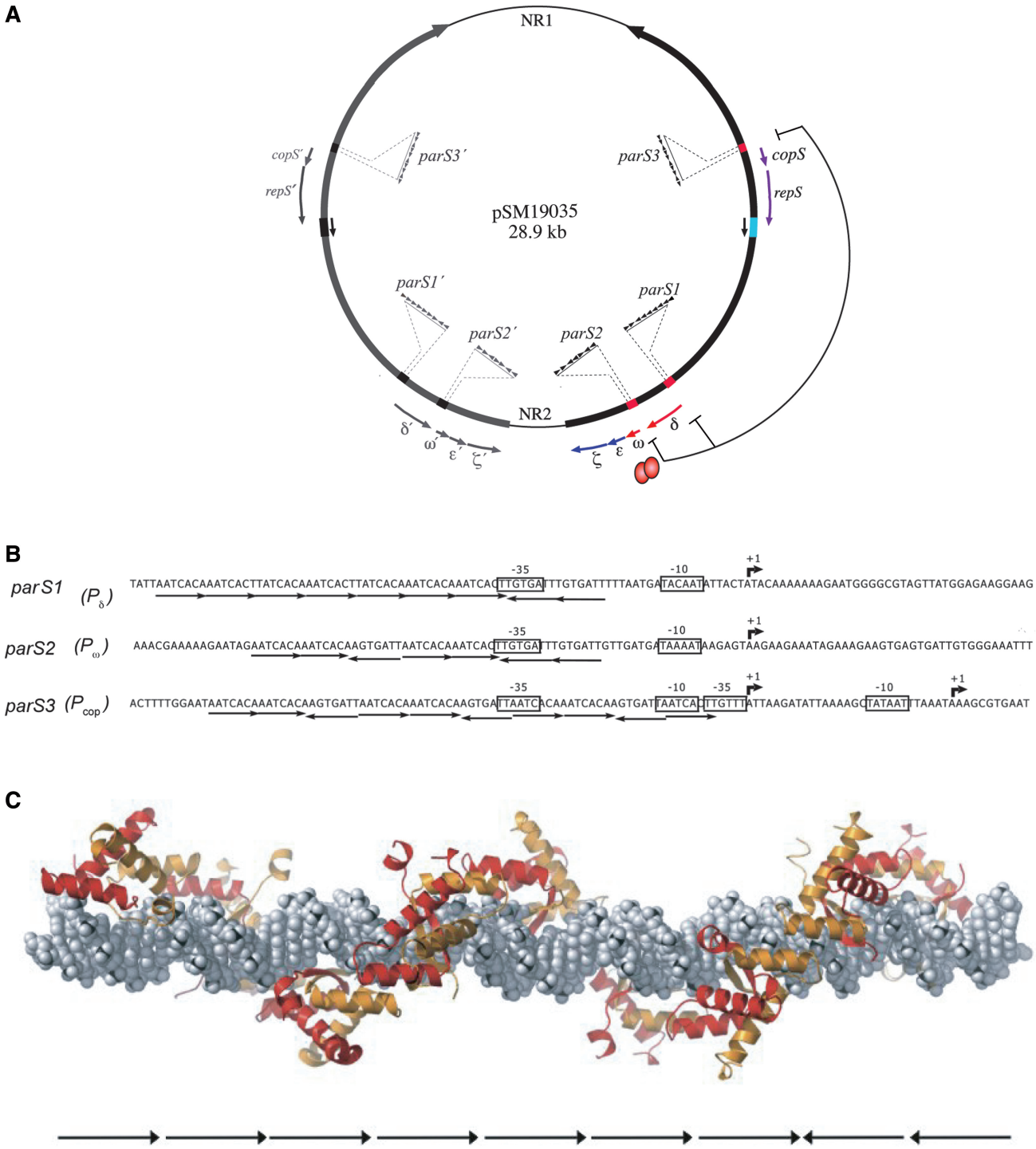

Figure 1. Genome organization and proposed structure of the ω_2•*parS* complex. (**A**) pSM19035 map. Duplicated sequences are indicated by the thick line, and unique non-repeated (NR) sequences by the thin line. The arrowheads on the thick lines denote the arbitrarily chosen polarity of the inverted repeated sequences. One arm of the repeated region is denoted in grey and is not described. The outer thin arrows indicate the replication and segregation loci. The replication origin (light blue box) and direction of replication (denoted by inner arrows) are indicated. The upstream region of the promoters of *copS*, δ and ω genes (red boxes), which constitute the six *cis*-acting centromere-like *parS* sites, are enlarged. The variable number of contiguous 7-bp heptad (iterons) repeats are symbolized by direct or inverse filled triangle. The promoters repressed by ω_2 (red balls) are indicated. (**B**) The *parS* sites consist of a variable number of contiguous iterons with the sequence 5′-WATCACW-3′, where W is A or T. The boxes denote the −35 and −10 boxes of the promoters of the *copS*, δ and ω genes, and the bent arrows denote the +1 of the transcripts. (**C**) The structural model of ω_2 bound to *parS*1 DNA. The overall structure of the PC (ω_2•*parS* DNA), with ω_2 forming a left-handed matrix around straight DNA is shown. The iterons are denoted as arrows.

of them decorates the nucleoid. In the presence of their ParB counterpart, ParAs are re-located, moving along and even between nucleoids (10–16). This oscillation of the ParA proteins is similar to that observed with MinD which oscillates between the cell poles in association with the membrane (17). Deconvolution of oscillation images suggests that: (i) ParB proteins dynamically regulate ParA oscillation; (ii) the ParA proteins form spiral structures on DNA; and (iii) ParA mutations which block ATP binding prevent nucleoid association (11–14,18).

Segregation of pSM19035 requires a type Ib ParAB system, composed of the NTPase δ_2, the CBP ω_2 and two sets of three *parS* centromere sites [(3,12,19), Figure 1A and B], comprising 9, 7 and 10 contiguous heptads of sequence 5′-WATCACW-3′ (where W is an A or a T) in direct or inverse orientation [(3,12,19), Figure 1B]. These *parS* sites overlap the promoter region of the δ, ω and *copS* genes, respectively [(3,20), Figure 1B].

The ω monomer is a 71-residue polypeptide with an unstructured N-terminal domain (residues 1–19) and a ribbon–helix–helix-fold (residues 20–71) (21–23). The N-terminal domain of ω is dispensable for regulation of plasmid copy number and of *par* and TA module expression (24,25) but essential for active partitioning; it is through this domain that the dimer form (ω_2) interacts with the ATPase dimer, δ_2 (12,26). Protein ω_2 or its variant $\omega_2\Delta$N19, which lacks the first 19-residues, binds with high affinity and cooperativity to *parS* DNA, with a ω_2:heptad stoichiometry of 1 (3,19,25). The crystallographic structures of $\omega_2\Delta$N19 in complex with two repeats in direct or inverted orientation and AFM analysis of ω_2•*parS* complexes have allowed us to propose the architecture of the partition complex (PC) [(24,26) Figure 1C]. In this complex, the ω_2 DNA-binding site faces inward, and successive ω_2 molecules are displaced relative to their neighbours by 7-bp so as to assemble as a left-handed helix that wraps around *parS* DNA, without bending or twisting it [(24,26), Figure 1C]. The PC formed by ω_2 do not spread significantly beyond the *parS* site, unlike those formed by large CBPs such as P1-ParB and F-SopB or the medium-sized CBP Spo0J of *Bacillus subtilis* that spread in a sequence-independent manner up to several kilobases upon binding to their cognate site(s) (27–30).

The δ_2 ATPase, whose monomer is a 284-residue long polypeptide, is essential for better-than-random plasmid segregation (1,12). In the presence of ATP•Mg^{2+}, δ_2 binds DNA in a sequence-independent manner (12). Note that unless stated otherwise the δ_2 ATPase or its mutant variants are in the ATP-bound form and denoted as δ_2, δ_2D60A, δ_2K242A, δ_2K248S or δ_2K259A/K260A, respectively.

The ω_2•δ_2 interactions are key events of the partition mechanism, but *in vitro* analyses have shown the outcome to depend on the ratio of the two proteins. At low ω_2:δ_2 ratios, ω_2 bound to *parS* enhances the ATPase activity of δ_2 and promotes plasmid pairing (26). At equimolar ω_2:δ_2 ratios, ω_2 stimulates ATP hydrolysis by δ_2 and promotes disassembly of the paired complexes (12). At high ω_2:δ_2 ratios, ω_2 promotes δ_2 polymerization onto DNA (12). In the ATP bound form, the small ATPases (δ_2, Soj, etc. 260 ± 50 residues long) and the *Vibrio cholerae* large ATPase ParA2, bind and polymerize on DNA in a sequence independent manner (12,31,32). In contrast, when bound to ATP, the large ATPases (370 ± 50 residues long) and few small ATPases, as ParF of pTP228 or ParA of pB171, form bundles of polymers in the absence of DNA or any other surface (33–38).

Cytological studies have shown that ParA binding to DNA and interaction with ParB, mediates pairing and plasmid movement in opposite directions (12,14–16,18,39,40). Indeed, the interaction of CBP bound to its cognate site with nucleoid-bound NTPase causes the re-localization of the latter *in vivo* (12,15,16,18,26). Atomic force microscopy (AFM) revealed that δ_2 bound to DNA non-specifically, was detached from DNA upon interaction with the PC and relocalized to form the segrosome complex (SC, Figure 2E) (26). Interaction of two SCs via δ_2 then forms a bridging complex (BC, Figure 2E) (12,26). The following step of unpairing, δ_2 polymerization on and depolymerization from DNA require ATP hydrolysis (12,26). Protein δ_2D60A, which binds but does not hydrolyse ATP, led to accumulation of BCs (Figure 2D and E), but Apo-δ_2K36A, which neither binds nor hydrolyses ATP, did not bind DNA (12,26).

To elucidate the early stages of pSM19035 partitioning we performed detailed biochemical analyses of these protein–DNA complexes. We report here that the paired partition complexes presumably needed to initiate plasmid segregation are not formed by random collisions of freely diffusing molecules but are constructed through a series of defined stages. Such deliberate assembly could facilitate regulation of partition in accordance with conditions prevailing in the cell.

MATERIALS AND METHODS

Chemicals, enzymes, proteins, DNA and reagents

All chemicals were p.a. grade and purchased from Roche Diagnostics (Mannheim, Germany). DNA restriction, DNA modification enzymes and nucleotides were from Boehringer (Mannheim, Germany). Ultrapure acrylamide was from Serva (Heidelberg, Germany). The broad protein molecular weight marker was obtained from GIBCO-BRL (Barcelona, Spain). Proteins ω_2, $\omega_2\Delta$19, ω_2T29A, δ_2, δ_2K36A and δ_2D60A and pBC30-borne *parS*2 DNA, which is the source of *parS* DNA, were purified as described (3,12,25). Similar results were obtained with the three *parS* sites (12,26, data not shown). Here, only experiments with *parS*2 DNA containing seven contiguous iterons or heptads, herein *parS* DNA, are described. Plasmid pCB746-borne δ gene was used for site-directed mutagenesis: AAA codons 242, 248 or 259 and 260 of wild-type (wt) δ gene coding for Lys, were exchanged for GCA, which encodes for Ala, or TCA encoding Ser. The His-tagged protein variants δ_2D211A, δ_2K242A, δ_2K248S or δ_2K259AK260A were purified as described for wt protein (12). The concentration of DNA was expressed as moles of DNA molecules and was determined using a molar extinction coefficient of 6500 M^{-1} cm^{-1} at 260 nm. The protein concentrations were determined by absorption

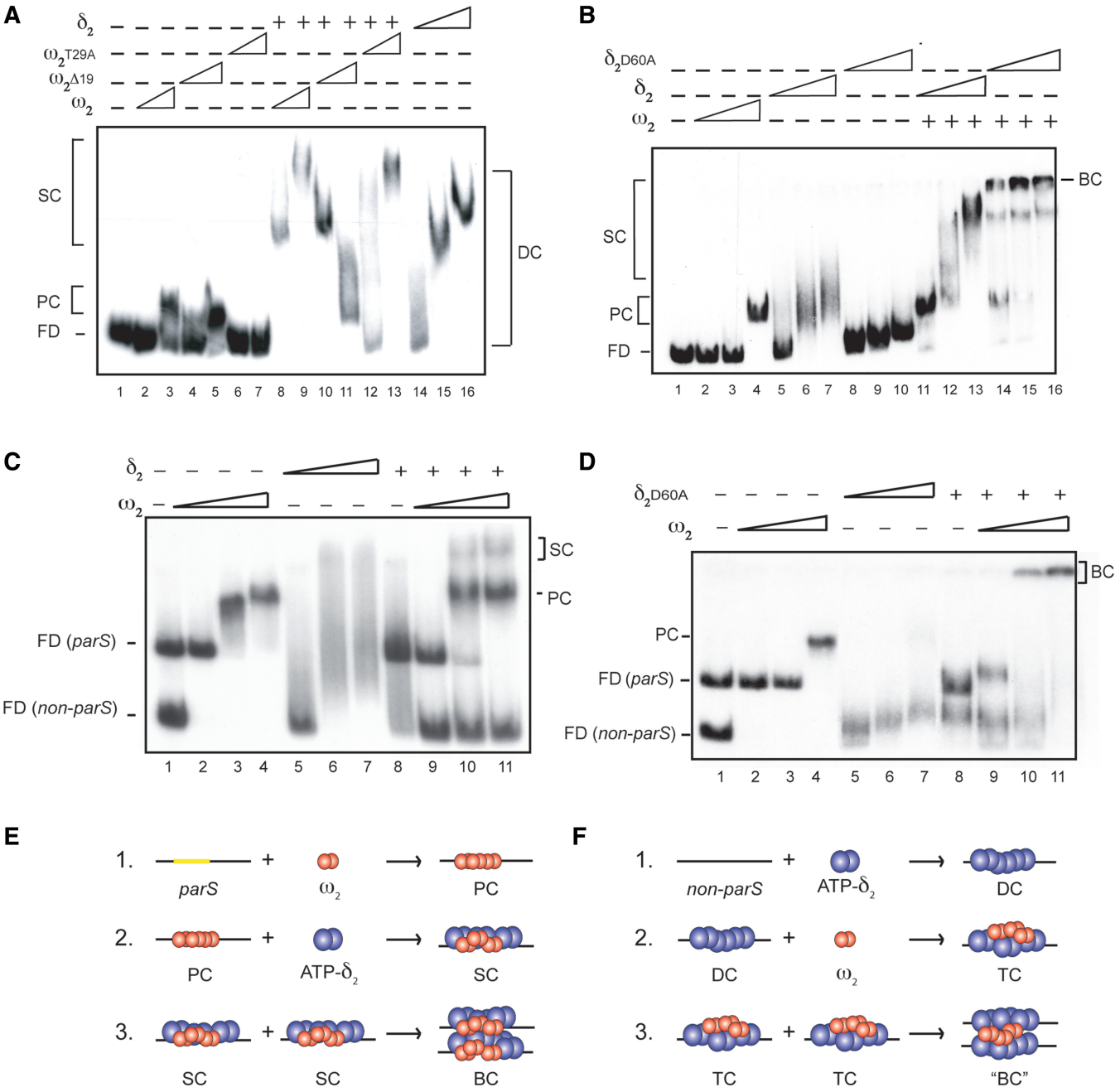

Figure 2. Complexes formed by ω_2 and δ_2 binding to *parS* DNA. (**A**) The 423-bp [α^{32}P]-*Hin*dIII-*Kpn*I *parS* DNA (0.1 nM) was incubated with increasing concentrations of ω_2 (3 and 6 nM), $\omega_2\Delta$N19 (4 and 8 nM), ω_2T29A (5 and 10 nM), δ_2 (140, 280 and 560 nM) or in the presence of δ_2 (140 nM, indicated by plus) and increasing amounts of ω_2, $\omega_2\Delta$N19 or ω_2T29A. (**B**) *parS* DNA (0.1 nM) was incubated with increasing amounts of ω_2 (1.5, 3 and 6 nM), δ_2 (140, 280 and 560 nM), δ_2D60A (35, 70 and 140 nM) or a constant amount of ω_2 (1.5 nM, indicated by plus) and increasing concentrations of δ_2 or δ_2D60A. (**C**) The 183-bp [α^{32}P]-*Bam*HI-*Hin*dIII *non-parS* DNA (0.1 nM) was incubated with increasing concentrations of δ_2 (120, 240 and 480 nM, lanes 5–7) or the 423-bp [α^{32}P]-*parS* DNA (0.1 nM) with increasing concentrations of ω_2 (3–12 nM, lanes 2–4). *non-parS* DNA was pre-incubated with δ_2 (120 nM) and then *parS* DNA and increasing concentrations of ω_2 (3–12 nM) were added. (**D**) n*on-parS* DNA was incubated with increasing concentrations of δ_2D60A (37, 75 and 150 nM, lanes 5–7) or *parS* DNA with increasing concentrations of ω_2 (3–12 nM, lanes 2–4). *non-parS* DNA was pre-incubated with δ_2D60A (75 nM) for 5 min, and then *parS* DNA and increasing concentrations of ω_2 (3–12 nM) were added and the reaction incubated for 15 min at 37°C in buffer A containing 1 mM ATP. The absence of a component is indicated by minus, and the presence of a fixed amount by a plus or variable concentration by a triangle, respectively. (**E**) Protein ω_2 bound to *parS* DNA led to the formation of a partition complex (PC); δ_2 bound to PC led to segrosome complex (SC) formation; and the interaction of two SCs led to bridging complex (BC) formation. (**F**) Protein δ_2 bound to DNA leading to dynamic complex (DC) formation; ω_2 binding to DC led to a transient complex (TC); and the interaction of two TCs led to pseudo-bridging complex ('BC') formation. FD, protein-free DNA.

at 280 nm using molar extinction coefficients of 2980 M^{-1} cm^{-1} for ω_2, $\omega_2\Delta$N19 and ω_2T29A, and 38 850 M^{-1} cm^{-1} for δ_2, δ_2K36A, δ_2D60A, δ_2D211A, δ_2K242A, δ_2K248S or δ_2K259A/K260A. Concentrations are expressed as mol of protein dimers.

Limiting proteinase K (ProK, 0.5–2 μg/ml) was used to partially proteolyse free δ_2 or DNA-bound δ_2, and the resulting products were separated using 15% SDS–polyacrylamide gel electrophoresis (PAGE). Tryptic digestion of gel-purified protein bands and their spotting onto the MALDI-targets (Voyager DE-STR, PerSeptive Biosystems, Foster City, USA) were performed as described (41). The MALDI-TOF-TOF measurements of spotted peptide solutions were carried out on a Proteome-Analyzer 4700 (Applied Biosystems, Foster City, USA) as described previously (41).

Protein–DNA complexes

For electrophoretic mobility shift assays (EMSA), gel-purified 423-bp [α^{32}P]-HindIII-KpnI *parS* DNA or 183-bp [α^{32}P]-BamHI-HindIII *non-parS* DNA (0.1 nM) was incubated with various amounts of wt ω_2 (or its variants), wt δ_2 (or its variants), or both proteins in buffer A (50 mM Tris–HCl pH 7.5, 10 mM $MgCl_2$, 50 mM NaCl) containing or lacking 1 mM ATP or ADP for 15 min at 37°C in 20 μl final volume as previously described (3,12). The reaction was stopped by addition of loading buffer (1 mM EDTA, 0.1% [v/v] bromophenol blue and 0.1% [v/v] xylene cyanol) and was then separated using 4 or 6% PAGE. PAGE conducted in running buffer was 1 × TAE at 45 V at 4°C, and the gels were dried prior to autoradiography as described (3).

DNase I footprinting was performed as previously described (3,19). Briefly [α^{32}P]-HindIII-KpnI *parS* DNA (1 nM) was incubated with wt ω_2 (or its variants), δ_2 (or its variants) or both proteins under the same conditions as the EMSA experiments (3,19). After 15 min incubation at 37°C, the footprint was started by DNaseI addition. After 2 min, the reactions were stopped by addition of loading buffer, separated in 6% denaturing (d) PAGE and autoradiographed. As size control markers, ladders obtained with the chemical sequencing reaction (G+A) for the same DNA fragments were used as described (19). Image analysis of the protein–DNA complexes and determination of length and volume of the complexes were measured by AFM as previously described (26).

To obtain apparent dissociation constant (K_{Dapp}) values from EMSA and DNase I footprint experiments, the concentration of free DNA and protein–DNA complexes was densitometrically determined under non-saturating conditions from differently exposed autoradiographs of EMSA and DNase I footprinting gels. Protein concentrations that transfer 50% of the free labelled DNA into complexes or protect 50% from DNase I digestion are approximately equal to the K_{Dapp} under conditions where the DNA concentration is much lower than the K_{Dapp}.

To determine the dissociation half-life of protein–DNA complexes, protein were incubated with [α^{32}P]-HindIII-KpnI *parS* DNA in buffer A containing 1 mM ATP, when indicated, for 15 min at 37°C in a 100 μl final volume as previously described (3,12). A 50-fold excess of unlabelled DNA was then added to the preformed protein–DNA complexes, and samples were collected at varying times and the solution was filtered through a nitrocellulose membrane filter (Millipore, type HAWP 0.45 μm) as previously described [(42), Supplementary Figure S1]. While free DNA passed through the filter the radiolabelled DNA bound to the protein was retained on the filter (42). Filters were dried and the amount of radioactivity bound to the filter was determined by scintillation counting. The DNA retained on filter was corrected for the retention of radiolabelled DNA in the absence of protein. The specific activity of the input labelled DNA was measured as 10% trichloroacetic acid precipitable material.

RESULTS

Protein ω_2 forms a discrete complex on *parS* DNA while δ_2 non-specifically binds DNA

To elucidate features of the early stages of plasmid segregation, the binding of ω_2 to centromeric *parS* DNA was studied. In the presence or absence of ATP, ω_2 bound with high affinity and specificity to *parS* DNA (K_{Dapp} ~5 ± 1 nM) to form a partition complex (PC) (Figure 2A, lanes 2 and 3; and Figure 2B–D, lanes 2–4). The PC formed was confirmed by AFM (Figure 2E and Supplementary Figure S2A). Protein $\omega_2\Delta$N19, which lacks the first 19-residues, bound *parS* DNA with similar affinity (K_{Dapp} ~7 ± 1 nM) (Figure 2A, lanes 4 and 5), but the ω_2T29A variant (Figure 2A, lanes 6 and 7), which contains an essential mutation in the DNA binding motif, bound *parS* DNA with low affinity (K_{Dapp} ~1.5 μM) (25). Proteins ω_2, $\omega_2\Delta$N19, or ω_2T29A, bound non-specific (*non-parS*) DNA with similar low affinity (K_{Dapp} ~1.5 μM) (24,25).

It has previously been shown that in their apo form, Apo-δ_2 or Apo-δ_2D60A failed to bind or to polymerize onto DNA in the nM range [(12), $K_{Dapp} > 1.5$ μM]. Similar results were observed when the proteins were in the ADP bound form (ADP-δ_2 or ADP-δD60A_2) (12). Protein δ_2 bound cooperatively to *parS* or *non-parS* DNA with similar affinity (Figure 2A–C, K_{Dapp} 150 ± 10 nM). Protein δ_2 formed a diffuse complex with DNA (Figure 2B, lanes 5–7). In contrast, δ_2D60A, which binds, but does not hydrolyse ATP (12), bound DNA with a 3- to 4-fold higher affinity than wt δ_2, leading to formation of discrete complexes (Figure 2B, lanes 8–10, K_{Dapp} 40 ± 6 nM).

To explain the differences of the K_{Dapp} of both proteins, we hypothesize that either δ_2D60A binds DNA faster than δ_2 or the latter protein upon ATP hydrolysis increases the off rate leading to a dynamic association and dissociation complex (DC, δ_2•DNA). To address these possibilities, δ_2 or δ_2D60A, at K_{Dapp}, were pre-incubated with *parS* DNA, and the half-life of the preformed complex was measured in the presence of a 50-fold excess of cold *parS* DNA as competitor by filter binding assays. When the cold DNA was omitted, there was no apparent time-dependent decrease in the protein•*parS* DNA complexes (data not

shown). As shown in Supplementary Figure S1, the time-dependent decrease of the retained *parS* DNA was used to calculate the half-life of protein–DNA complexes. The half-life of δ_2•DNA was ~10 min, which was ~3-fold longer for the δ_2D60A•DNA complex (~28 min). It is likely that: (i) δ_2 binding to DNA specifically requires ATP; (ii) δ_2 and δ_2D60A bind DNA with similar affinities and (iii) ATP hydrolysis makes the short δ_2·DNA filament dynamic, leading to DC formation (Figure 2A). The DC formed was confirmed by AFM (Figure 2F and Supplementray Figure S2B).

Proteins ω_2 and δ_2 bind *parS* DNA forming a ternary complex

Stable physical interactions in solution have not been detected between δ_2 and ω_2 (12). To determine whether *parS* DNA, δ_2 and ω_2 (or its variants, $\omega_2\Delta$N19 or ω_2T29A) formed ternary complexes, EMSA studies were performed. In the presence of *parS* DNA, sub-saturating ω_2 (2- to 4-fold lower than K_{Dapp}) and saturating δ_2 (2- to 4-fold higher than K_{Dapp}) concentrations formed a low-mobility complex, termed the segrosome complex (SC) (Figure 2A, lane 9; and Figure 2B, lane 13). SC formation was confirmed by AFM analysis (Figure 2E). When the ω_2T29A variant, which does not bind DNA at the range of concentrations tested here, replaced wt ω_2, the slow moving complex also accumulated (Figure 2A, lane 13). However, when the $\omega_2\Delta$N19 variant, which binds *parS* DNA but fails to interact with δ_2, was used, only diffuse low-mobility DC was observed (Figure 2A, lanes 10 and 11). It is likely that DNA-bound δ_2 loads both ω_2 onto *parS* DNA and ω_2T29A onto DNA but fails to interact with $\omega_2\Delta$N19.

At ω_2 concentrations below K_{Dapp} (e.g. 1.5 nM), formation of PCs (ω_2•*parS* DNA) were not observed (Figure 2B, lane 2), but in the presence of limiting δ_2 or δ_2D60A concentrations, PCs were readily formed (Figure 2B, lanes 11 and 14). Sub-saturating or saturating δ_2 concentrations increased ternary complex formation (ω_2•*parS*•δ_2) and led to the accumulation of SC (Figure 2B, lanes 12 and 13). High-order complexes, formed by two or more SCs, leading to BC, were also confirmed by AFM analysis (Figure 2E and Supplementary Figure S2C). Unlike wt protein, δ_2D60A accumulated bands that migrated slower (BC; Figure 2B, lanes 14–16). Although ω_2 shows significantly greater binding affinity when compared to δ_2 or δ_2D60A, it appears that the latter two were able to markedly enhance the affinity of ω_2 for *parS* DNA. It is likely that both ω_2 and δ_2 interact and cooperate to circumvent the energetic and spatial constraints required for ω_2 binding to *parS* DNA.

Protein ω_2 binding to *parS* DNA promotes dislodging of DNA-bound δ_2

Previous studies revealed that δ_2 is an ATP-dependent DNA binding protein whose activities are controlled by ω_2 (12). To re-evaluate the hypothesis that δ_2 interacts with ω_2 and facilitates the interaction with *parS* DNA, EMSA studies were performed with *parS* and *non-parS* DNAs. Protein δ_2 or δ_2D60A was pre-bound to *non-parS* DNA (Figure 2C and D, lanes 5–7), and then preformed ω_2•*parS* DNA was added to the reaction mixture. Protein δ_2 or δ_2D60A pre-bound to *non-parS* DNA interacted poorly with *parS* DNA (Figure 2C and D, lane 8). At limiting ω_2 concentrations, δ_2 was dislodged from *non-parS* DNA (Figure 2C, lanes 8 and 9). At sub-saturating ω_2 concentrations, the PC and SC accumulated (Figure 2C, lanes 10 and 11), suggesting that ω_2 bound to *parS* DNA promotes the re-localization of δ_2 towards *parS* DNA to form a SC, as shown by the accumulation of free *non-parS*, and the slow moving SCs (Figure 2C). However, when wt δ_2 was replaced by δ_2D60A, the accumulation of free *non-parS* DNA was decreased (Figure 2D), suggesting that dislodging might require ATP hydrolysis. Under this condition, the accumulation of BCs was observed. It is possible that proteins bound to both DNA molecules led to BC formation, where two or more SCs paired (Figure 2D, lanes 10 and 11; and Figure 2E). The formation of BCs was confirmed by AFM analysis (26).

Protein ω_2 binding to *parS* DNA promotes δ_2 re-localization

To further evaluate whether both proteins interact and ω_2 promotes re-localization of δ_2, enzymatic footprinting experiments were performed. Binding of ω_2 or $\omega_2\Delta$N19 to DNA specifically protected *parS* sequences from DNase I cleavage, with only limited spreading (<15 nt) on non-specific sequences (Figure 3A, lanes 6, 8 and 10). At limiting protein concentrations (seven δ_2/ *parS* DNA molecule), a globular-shaped δ_2 bound DNA in a sequence-independent manner (Supplementary Figure S2B). In contrast, at saturating protein concentrations (>75 protein molecules/ *parS* DNA molecule), δ_2 or δ_2D60A polymerized onto *parS* DNA and protected extended regions from DNase I digestion in a concentration-dependent manner (Figure 3A, lane 4; and Figure 3B, lanes 6 and 9).

When sub-saturating ω_2 concentrations were added to pre-formed DCs (δ_2•*parS* DNA complexes) the ω_2 cognate site became protected from DNase I, even in the presence of saturating δ_2 concentrations (Figure 3A, lanes 11 and 12; and Figure 3B, lanes 10–12). However, δ_2 bound to *parS* DNA was poorly re-localized by $\omega_2\Delta$N19 (Figure 3A, lanes 13 and 14), suggesting that specific contacts between δ_2 and ω_2 are determined by the N-terminal 18 amino acid residues of ω_2 (24,25). When sub-saturating ω_2 concentrations were added to pre-formed δ_2D60A•*parS* complexes, the ω_2 cognate site was also protected from DNase I. Protein ω_2 bound to *parS* DNA partially redistributed δ_2D60A next to it (Figure 3B, lanes 13–15). It is likely that ω_2 bound to *parS* DNA redistributes δ_2 to adjacent regions, to form a SC (Figure 2E, 26).

The DNA binding domain of δ_2 maps in its C-terminus

Recently it has been shown that the ParA-like proteins (e.g. pSM19035-δ_2, F-SopA, P1-ParA or chromosomal-encoded Soj) in the ATP bound form bind DNA through its C-terminus (12, this work, 31,32,36,43). To

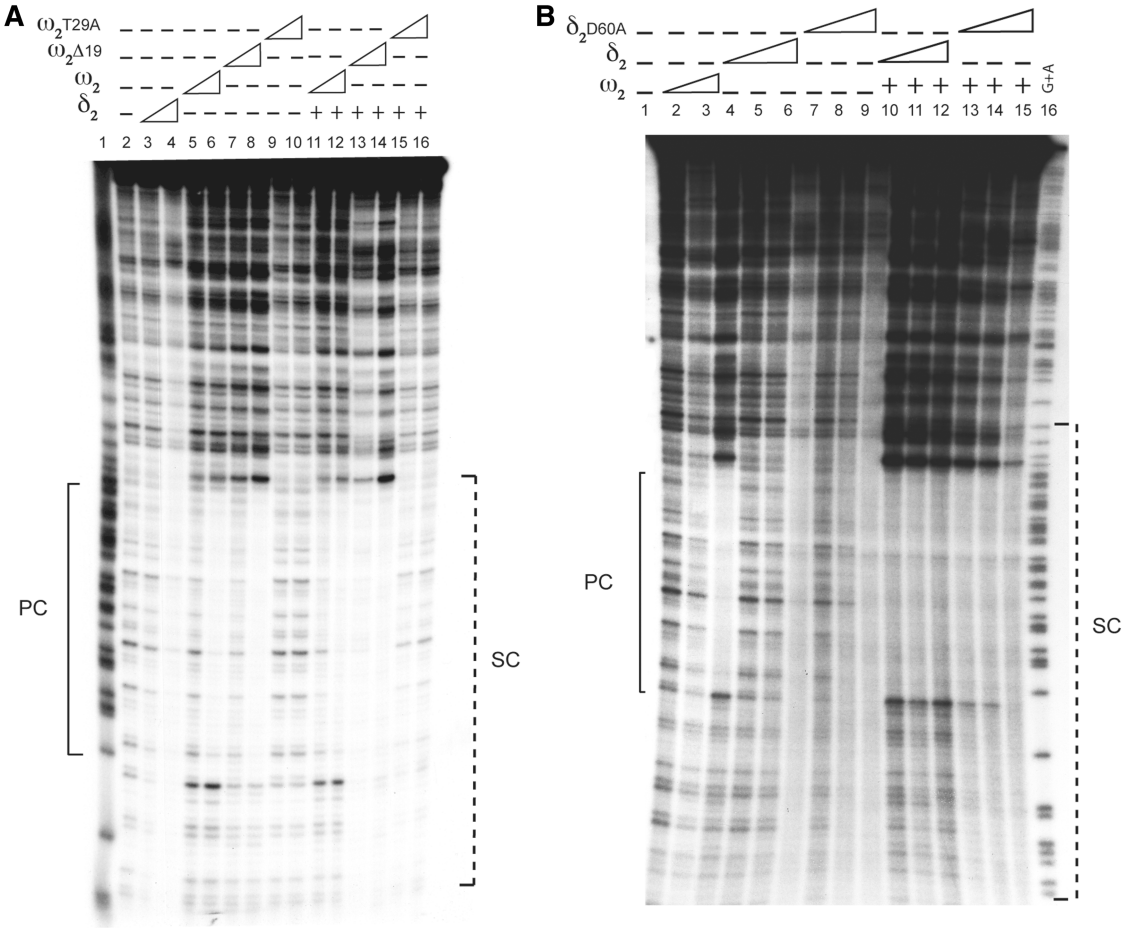

Figure 3. DNase I footprinting shows that ω_2 redistributes δ_2 to form a SC. (**A**) The 423-bp [α^{32}P]-HindIII-*Kpn*I *parS* DNA (1 nM, bottom strand) was incubated with δ_2 (75 and 140 nM), ω_2 (6 and 12 nM), $\omega_2\Delta$N19 or ω_2T29A (8 and 12 nM) or *parS* DNA was pre-incubated with a fixed concentration of δ_2 (280 nM), and then incubated with increasing concentrations of ω_2, $\omega_2\Delta$N19 or ω_2T29A. (**B**) *parS* DNA was incubated with δ_2 (140, 280 and 560 nM), δ_2D60A (35, 75 and 150 nM), ω_2 (6 and 12 nM), or a fixed concentration of ω_2 (12 nM) and increasing concentrations of δ_2 or δ_2D60A. DNase I was then added. In lanes 1 (A) and 16 (B) the size standard G + A was loaded. The DNA regions protected from DNase I digestion by ω_2, δ_2 or both are denoted. The abbreviations used are those defined in Figure 2.

define functional δ_2 regions and to examine whether binding to DNA protects structural domains of δ_2, limited proteolysis together with mass spectrometry experiments were performed. Limited ProK proteolysis, of δ_2 unbound or DNA-bound, revealed that the C-terminal fragment (band d) became less sensitive to ProK digestion upon DNA binding (Figure 4A, lanes 3, 5 and 7). The N-terminal folded core (band a) of δ_2 became more sensitive to proteolysis in the DNA bound form (Figure 4A, compared bands a, b and c). Limiting trypsinolysis of the gel-purified a–d polypeptide bands in conjunction with mass spectrometry analysis allowed us to identify these bands (Figure 4B). The polypeptide stabilized in the presence of DNA corresponded to the C-terminal end (Figure 4B). A structural comparison of these regions from different ATPases revealed that there are charged residues, but they are poorly conserved (Figure 4C). An analysis of the residues implicated in ATP-Soj$_2$, P1-ATP-ParA$_2$ or F-ATP-SopA$_2$ sequence-independent DNA binding (32,36,43) and the surface-exposed charged residues of δ_2 suggested a potential role for residues D211, K242, K248 and K259/K260 in DNA binding. These residues were replaced by Ala or Ser, and the resulting products were purified and biochemically analysed. In the ATP-bound form, the δ_2 variant D211A had undiminished sequence-independent DNA binding relative to wt δ_2 (data not shown). As revealed in Figure 4D, the δ_2K242A mutant bound DNA with ~30-fold lower affinity ($K_{Dapp} > 3\,\mu M$) relative to wt δ_2. Similar results were observed with the δ_2K248S or δ_2K259A/K260A variants (data not shown). The DNA binding defect presented by δ_2K242A, δ_2K248S or δ_2K259A/K260A was specific because all of them formed dimers in solution and were able to bind and hydrolyse ATP (data not shown), suggesting that these mutants were properly folded.

Interaction of δ_2 with ω_2 markedly increases PC formation

Previously, it was assumed that ω_2 was present in two molecular states, *parS*-bound and free in the cytosol, and that all molecules in the system were competent for *parS* binding (19,24). Protein ω_2 specifically bound *parS* DNA with a K_{Dapp} ~5 ± 1 nM, but no binding to *parS*

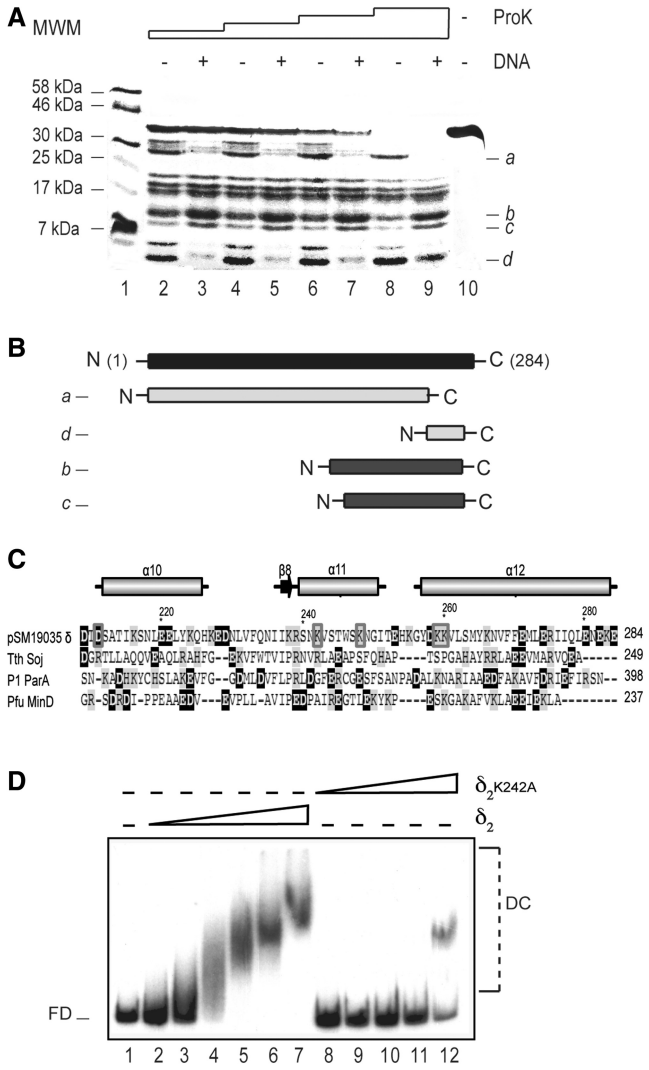

Figure 4. The δ_2 DNA binding domain maps to its C-terminus. (**A**) Partial proteolysis assays. Protein δ_2 (4 μg) was pre-incubated (+) or not (−) with the 423-bp *parS* DNA. Increasing concentrations of ProK were added and the mixtures were analysed by 15% SDS–PAGE. In lane 1 the molecular weight marker and in lane 10 untreated δ_2 are shown. The relevant proteolysis bands are marked (a–d). (**B**) Identification of relevant polypeptides. The polypeptides were isolated (bands a–d), subjected to partial proteolysis and mass spectrometry and the corresponding regions are labelled. The sequence coverage of the indicated polypeptide was: a, 48%; b, 39%; c, 27%; and d, 43%. (**C**) Conservation of charged residues in C-terminal segments of ATPases as Soj of *T. thermophilus*, P1-ParA and *P. furiosus* MinD. The residue numbering and the secondary structures are derived from δ_2. The changed residues are boxed in grey, and the negatively (boxed in black) and positively charged residues (boxed in grey) are highlighted. (**D**) The 423-bp [α^{32}P]-*parS* DNA (0.1 nM) was incubated with increasing amounts of δ_2 (0.035–1.2 μM) or δ_2K242A (0.3–4.8 μM) for 15 min at 37°C, in buffer A containing 1 mM ATP. FD, indicates protein-free DNA; DC indicates the protein–DNA complexes.

DNA was observed at limiting (<2 nM) concentrations (Figure 5A, lanes 2 and 3). Limiting concentrations of Apo-δ_2 or Apo-δ_2D60A failed to bind *parS* DNA (Figure 5A, lanes 6–11). To determine whether δ_2 increases PC formation EMSA studies were performed. Apo-δ_2 or Apo-δ_2D60A increased formation of ω_2•*parS* DNA complexes at least 6- to 8-fold (Figure 5A, lanes 13, 14, 16 and 17). In this experiment, we cannot rule out that δ_2 or δ_2D60A formed transient complexes with DNA in the presence of ω_2 and that such interaction increases the accumulation of PCs. To test this hypothesis, δ_2 was replaced by δ_2K242A, which is deficient in DNA binding (Figure 4D). In the presence of limiting ω_2 concentrations (~6-fold lower than the K_{Dapp}), addition of Apo-δ_2K242A (or δ_2K242A at ~100-fold lower than the K_{Dapp}) facilitated ω_2 binding to *parS* DNA (Figure 5B, lanes 11–13, K_{Dapp} 0.7 ± 0.1 nM). Similar results were observed when δ_2K36A, which cannot bind or hydrolyse ATP nor bind DNA, was used (data not shown). It is likely that a transient and synergistic interaction between δ_2 and ω_2 increases the ω_2 K_{Dapp} at least ~7-fold, and such an effect occurs even in the absence of Apo-δ_2 binding to DNA. It is worth mentioning that: (i) ω_2 binds its cognate site with a stoichiometry of 1 (19,24), (ii) the *parS* used contains seven heptads, and in the above experiments the *parS* concentration was 0.1 nM, suggesting that the K_{Dapp} could be even smaller and (iii) the ω_2•δ_2 interaction, which might also involve determinants in the C-terminal region of δ_2, was not affected by the K242A mutation in δ_2.

To address whether δ_2 or its variant increased the on or off rate of the reaction, the dissociation rate of the ω_2•*parS* was measured both in the presence or absence of δ_2K242A. Previously, it was shown by surface plasmon resonance that the ω_2•*parS* complex is short-lived (~50 s) (19). *parS* DNA was incubated with half-saturating ω_2 concentrations (6 nM) or with ω_2 and Apo-δ_2K242A (100 nM). As expected, the half-life of the ω_2•*parS* complex was short-lived, but increased >10-fold to ~34 min in the presence of Apo-δ_2K242A (Supplementary Figure S3). Since the addition of Apo-δ_2K242A decreased the dissociation rate of the PC, it was assumed that Apo-δ_2 or Apo-δ_2K242A transiently interacted with the unstructured N-terminal domain of ω_2, facilitating domain folding and/or a more extended ω_2 structural change, leading to an ω_2 variant (ω_2*) with an structured N-terminal end. We suspect that upon a transient δ_2•ω_2 interaction, there are two PC states: a transient (PC1, ω_2•*parS* DNA, Figure 2E) and a stable (PC2, ω_2*•*parS* DNA, Figure 7) one.

To test whether limiting δ_2 or δ_2K242A concentrations also facilitated PC2 formation, EMSA experiments were performed. Protein δ_2 stimulated PC and SC formation (Supplementary Figure S4, lanes 13 and 14), whereas δ_2K242A could only stimulate PC2 formation (Supplementary Figure S4, lanes 16 and 17), suggesting that stable SC formation required δ_2 to interact with DNA.

The ω_2 and δ_2 interaction facilitates DC and TC formation on DNA

Previously, it was shown that: (i) at low ω_2:δ_2 ratios (0.3:1), ω_2 bound to *parS* DNA stimulates the ATPase activity of δ_2 and (ii) at high ω_2:δ_2 ratios (4:1), δ_2 polymerizes onto DNA (12). To re-evaluate the hypothesis that ω_2, at *parS*, promotes changes in δ_2 and facilitates

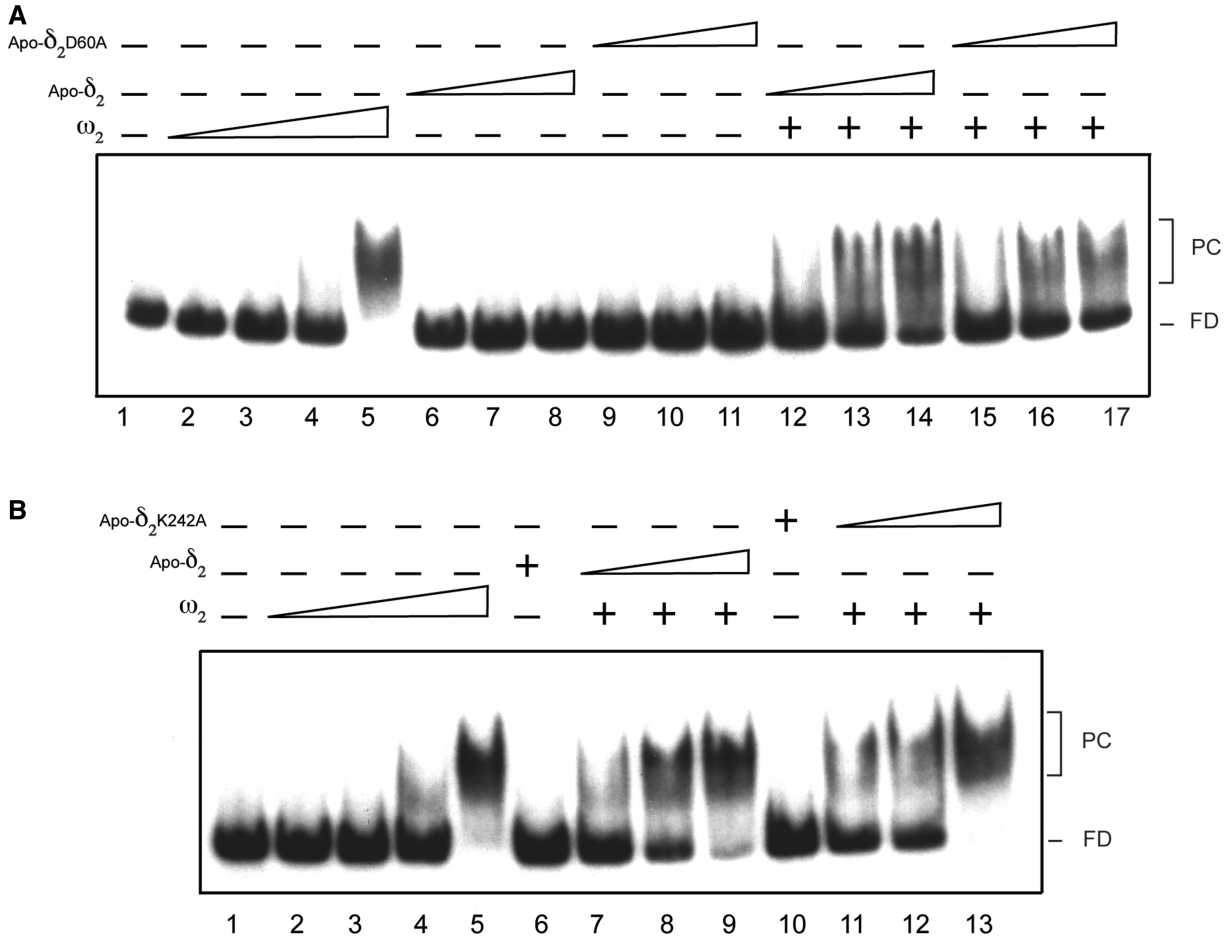

Figure 5. Apo-δ_2 facilitates ω_2•*parS* DNA complex formation. (**A**) The 423-bp [α^{32}P]-*Hin*dIII-*Kpn*I *parS* DNA (0.1 nM) was incubated with increasing concentrations of ω_2 (0.75–6 nM), Apo-δ_2 or Apo-δ_2D60A (25, 50 and 100 nM), or in the presence of ω_2 (0.75 nM, indicated by plus) and increasing amounts of Apo-δ_2 or Apo-δ_2D60A for 15 min at 37°C in buffer A. (**B**) *parS* DNA was incubated with increasing concentrations of ω_2 (0.75–6 nM) or in the presence of a fixed amount of Apo-δ_2 or Apo-δ_2K242A (100 nM), or ω_2 (0.75 nM, indicated by plus) and increasing amounts of Apo-δ_2 or Apo-δ_2K242A (25, 50 and 100 nM) for 15 min at 37°C in buffer A. The abbreviations used are the same as those used in Figure 2.

SC formation, EMSA studies were performed with *non-parS* DNA. Limiting ω_2 (>250-fold lower than K_{Dapp} for non-specific DNA) did not bind DNA lacking its cognate site (Figure 6A, lanes 2–4), and δ_2, at sub-saturating concentrations, promoted DC formation (Figure 6A, lane 5). Addition of limiting ω_2 concentrations to pre-formed DC (Figure 2F) facilitated the formation of a slow-moving transient complex (TC) (Figures 2F and 6A, lanes 6–8). The TC, which resembles the SC, is a very transient complex formed in the absence of *parS* DNA. In the presence of both proteins and DNA a discrete band that moved slower than the TC was formed, this new complex appeared to be a pseudo BC and was termed 'BC' (Figure 2F). The accumulation of TC and 'BC' was less evident when limiting ω_2 concentrations were incubated with *non-parS* and followed by addition of limiting δ_2 concentrations (Figure 6B, lanes 6–9). Protein ω_2 did not increase the affinity of δ_2 for *non-parS* DNA (Figure 6B, lanes 9 and 13). The presence of both proteins on *non-parS* DNA (TC) and pairing of *non-parS* DNA molecules ('BC') were confirmed by AFM (26).

DISCUSSION

To gain insights into the molecular mechanisms that ensure the accurate distribution of a newly replicated genome to daughter cells at cell division by the type Ib ParAB system, the process was analysed in four different stages as summarized in Figure 7. First, ω_2 binding to *parS* DNA and δ_2 binding to non-specific DNA lead to transient PC1 and DC formation, respectively (Figure 7A, conditions 1 and 2). Second, the interaction between PC1 and Apo-δ_2 lead to the formation of a stable PC2, but PC2′s interactions with DNA-bound δ_2 leads to δ_2 re-localization of the DC towards PC2 and SC formation (Figure 7A, conditions 1 and 2). Third, the interaction of δ_2, in the SC, with a second SC leads to the formation of a dynamic BC (plasmid pairing complex) (Figure 7A, condition 2). Finally, ω_2-bound to *parS* stimulates the ATPase activity of δ_2, BC disassembly, and δ_2 polymerization (Figure 7B). ATP hydrolysis at the end of the filament led to ADP-δ_2 release from DNA. PC2 interaction with the new end of the filament moves the plasmid, like a cargo, towards the cells poles (Figure 7B). In previous

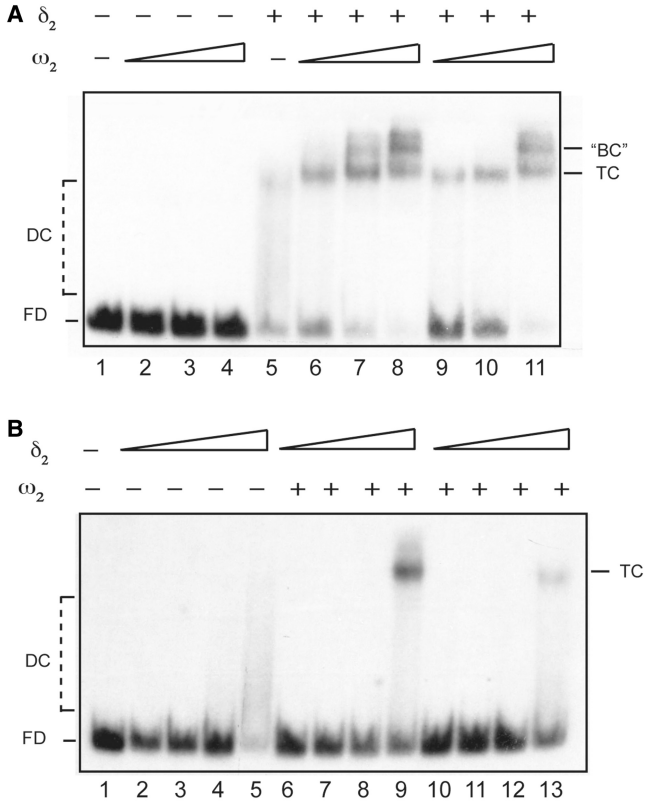

Figure 6. Protein ω_2 facilitates TC formation. (**A**) The 183-bp [α^{32}P]-BamHI-HindIII *non-parS* DNA (0.1 nM) was incubated with increasing concentrations of ω_2 (1.5, 3 and 6 nM). A fixed concentration of δ_2 (140 nM, indicated with plus) was pre-incubated with *non-parS* DNA (lanes 9–11) or increasing concentrations of ω_2 (1.5–6 nM, lanes 6–8), then incubated with increasing ω_2 concentrations or *non-parS* DNA, respectively. (**B**) [α^{32}P]-*non-parS* DNA (0.1 nM) was incubated with increasing concentrations of δ_2 (17, 35, 70 and 140 nM) for 15 min at 37°C in buffer A containing 1 mM ATP. Increasing concentrations of δ_2 were pre-incubated with *non-parS* DNA (lanes 6–9) or with a fixed amount of ω_2 (3 nM, lanes 10–13) and then incubated with a fixed amount of ω_2 (3 nM) or non-*parS* DNA, respectively, for 15 min at 37°C in buffer A containing 1 mM ATP. The abbreviations used are the same as those used in Figure 2.

reports, the late stages (dynamic plasmid pairing, and polymerization and de-polymerization) of pSM19035 partitioning were addressed (12,26). In this report we have dissected the early stages, the transient and the stable PCs, SC, DC, TC and BC formation, leading to pSM19035 partitioning (Figure 7A).

Protein δ_2 binds DNA

Limited proteolysis experiments revealed that δ_2 has several regions that become protected upon DNA binding, suggesting that DNA binding have local consequences and induce conformational changes in the protein (Figure 7, ATP-δ_2*). The residues required for non-specific DNA interaction in δ_2, ATP-Soj, or ATP-SopA are not conserved but map generally to the C-terminal region [(32,43), Figure 4]. Single point mutations in α11, as in residues K242 (δ_2K242A), abrogate DNA binding, without affecting protein dimerization or ATP hydrolysis (Figure 4D, data not shown). An equivalent mutation in Soj (e.g. ATP-Soj$_2$R218A), only marginally (2- to 2.5-fold) reduces the DNA binding affinity relative to wt ATP-Soj$_2$, but the ATP-Soj$_2$R218E variant shows no binding to DNA (32). These finding suggested that: (i) ATP induced transient δ_2 conformational change, which might be stabilized upon DNA binding and (ii) the basic residues in the C-terminal region contact the DNA phosphate backbone. Type Ia ParA ATPases, such as P1-ParA$_2$ or F-SopA$_2$, when bound to ATP, mediate segregation by interacting with *parS*-bound ParB (6–9). ATP-ParA$_2$ or ATP-SopA$_2$ also contains a basic region in the C-terminus that contacts DNA in a sequence-independent manner (36,43). This basic region of P1-ParA is equivalent to the DNA binding motif of δ_2. Indeed, the P1-ParA$_2$K375A/R378A double mutation, in the ADP bound form, essentially abrogated DNA binding (36). Similarly, the δ_2K259A/K260A variant also abrogates DNA binding (data not shown).

Like *B. subtilis* Soj or *V. cholerae* ParA2, δ_2 in concert with ω_2 bound to *parS* polymerizes on DNA forming nucleoprotein filaments (12,31,44). Interaction of δ_2 with DNA led to diffuse migrating bands that could be attributed to polymerization and subsequent depolymerization of DC by ATP hydrolysis. However, the interaction with limiting ω_2 facilitates TC formation on *non-parS* DNA (Figure 7A, condition 3). This is consistent with the observation that δ_2D60A, which binds but does not hydrolyse ATP, forms a stable *non-parS*•δ_2•ω_2•δ_2•*non-parS* DNA complex. However, ParF of pTP228 and the large ParA ATPases follow a different path, because these ATPases form bundles in the absence of any surface (15,35–37).

Protein δ_2 regulates the dynamics of PC formation

Centromere recognition in pSM19035 includes six copies of *parS* DNA containing several copies of unspaced iterons, and a small size CBP, ω_2 (19,23). *parS* DNA forms a transient complex with ω_2 (PC1), with high affinity and cooperativity. PC1 leads to a contiguous left-handed helical nucleoprotein complex that does not distort the contour length of right-handed *parS* DNA (24,26). DNA titration experiments with increasing numbers of iterons (heptads) and stoichiometric studies of the PC1 revealed that each iteron recruits one ω_2 molecule. Each ω_2 being displaced relative to its neighbour by 7-bp and left-handed rotated by 252° (19,24). The overall structure of the PC1, in linear or supercoiled DNA, revealed the formation of a discrete structure with ω_2 wrapping around straight B-form *parS* DNA, without significant spreading, compaction, shortening or distortion of the DNA (24,26). At the PC1, the ω_2 DNA-binding domain is facing inward (Figure 1C). The interaction of δ_2 or Apo-δ_2 with PC1 stimulate the assembly of the longer-lived PC2 (see below). Unlike ω_2-mediated PC1 or PC2 formation, the large (e.g. P1-ParB or F-SopB) and middle size (e.g. chromosomal-encoded Spo0J) CBPs, which recognize their cognate target via a helix-turn-helix domain, spread onto and around *parS* up to several kilobases of DNA in a centromere-dependent manner upon binding to *parS* DNA (27–30).

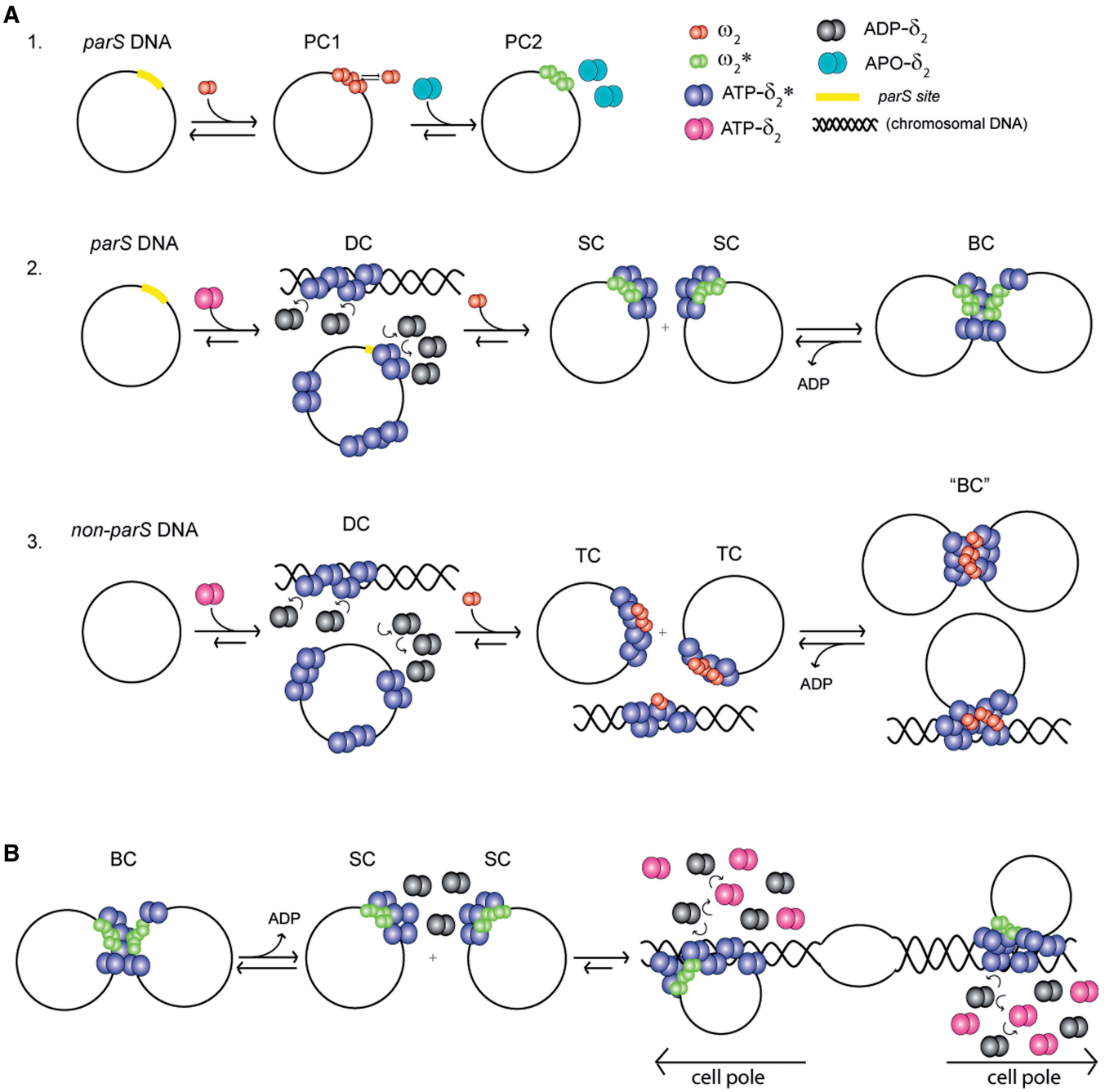

Figure 7. Dynamic assembly of different types of protein–DNA complexes. (**A**) (1) Protein ω_2, upon interaction with Apo-δ_2, δ_2K242A or δ_2, undergoes a conformational transition which enables ω_2* to bind *parS* DNA with high affinity and stability. (2) The interaction of δ_2 with any DNA has local consequences and induces conformational changes in the protein (ATP-δ_2*). Protein δ_2 interacts with DNA to promote DC formation. Protein ω_2*, at the PC2, promotes δ_2 redistribution towards the SC. δ_2, at *parS*, regulates SC and BC formation. Two or more SCs produce a large high-order complex (BC). (3) δ_2 promotes the formation of a DC on *non-parS* DNA. The interaction of δ_2, at the DC, with ω_2 facilitates TC formation and the accumulation of 'BC'. (**B**) Dynamics of plasmid pairing and plasmid segregation. Protein δ_2, at the DC, polymerizes onto DNA. ATP hydrolysis promotes disassembly of the BC with SC accumulation. The interaction of unpaired SC with the DC stimulates ATP hydrolysis, dislodges the 'BC' and promotes depolymerization of δ_2. The subsequent round of interaction of SC with the DC stimulates the retraction of the δ_2 filament and moves the plasmids away from each other (towards the cell pole).

We propose that δ_2 positively controls the dynamic activities of ω_2 on *parS* DNA. Protein ω_2 binds *parS* DNA to form PC1. A transient interaction between Apo-δ_2 and PC1 markedly stabilizes the latter (>12-fold) leading to the accumulation of the PC2 intermediate (ω_2*•*parS* DNA) (Figure 7A, condition 1), δ_2•PC1 interaction leads to SC and BC formation (Figure 7A, condition 2). This is consistent with the observations that: (i) the PC is a highly dynamic structure (with a PC1 half-life <1 min) (19) and (ii) the Apo-δ_2K242A or δ_2K242A

variant, which abrogates DNA binding, or Apo-δ_2K36A, which abrogates ATP binding and hydrolysis and DNA binding, markedly enhanced PC2 formation (Figures 5 and 7A, condition 1, data not shown). It is likely that ω_2 binds to *parS* DNA and forms the transient PC1. Therefore, the interaction of Apo-δ_2 or δ_2 with the unstructured N-terminal domain of ω_2 induces conformational changes in the latter to facilitate PC2, SC or BC formation, respectively. Unlike ω_2•*parS*, pB171-ParB binds to the centromere and forms discrete PCs and large, high-order complexes consisting of several DNA fragments joined by ParB at the centromere site (BC complex or plasmid pairing) in the absence of pB171-ParA (45).

Protein ω_2 facilitates SC and BC formation on *parS* DNA

We propose that ω_2 also controls the dynamic activities of δ_2. Different ω_2:δ_2 ratios and the presence of *parS* DNA play a critical role in the regulation of the different stages of plasmid segregation. At stoichiometric concentrations of both proteins ω_2 binding to *parS* DNA promotes dislodging of δ_2 from *non-parS* DNA and re-localization towards PC2 leading to SC and BC formation (Figures 2C and 7A, condition 2). It is likely that this dynamic redistribution resembles ParA oscillation from *non-parS* DNA (the nucleoid) to ParB-bound *parS* DNA. The δ_2•ω_2 interaction induces conformational changes in both proteins. The interaction of two SCs leads to the formation of a BC, with subsequent change in the ω_2:δ_2 ratios (12,26). Indeed, the unstructured N-terminal domain of ω_2 is required to control δ_2-medited ATP hydrolysis and formation of the transient SC and BC (Figure 7A, condition 2). The BC, which resembles specific plasmid pairing (26), was dislodged upon PC2 stimulated ATPase activity of δ_2, leading to SC formation (Figure 7B).

Protein ω_2 facilitates TC and 'BC' formation on *non-parS* DNA

At limiting protein concentrations, δ_2 binds cooperatively to DNA forming discrete bead-like transient DCs of variable length (26). Limiting ω_2 (>250-fold lower than K_{Dapp} for *non-parS* DNA), upon interaction with δ_2 bound to *non-parS* DNA facilitating TC and 'BC' formation (Figure 7A, condition 3). It is likely that δ_2, at the transient DC, should load ω_2 onto *non-parS* DNA. Indeed, δ_2-bound *non-parS* DNA (DC) facilitates ω_2 loading onto *non-parS* DNA, TC and 'BC' formation. However, in the presence of limiting ω_2 concentrations, only TC formation was detected. Formation of 'BCs', which have similar apparent mobility to that of genuine BCs at *parS* regions (Figures 2B and 6A), is dynamic, with ω_2 stimulating δ_2 release from *non-parS* DNA. The interaction of both proteins leads to BC on *parS* and 'BC' formation on *non-parS* DNA, suggesting a genuine interaction rather than a random collision of free particles. This is consistent with the observation that δ_2 facilitates plasmid pairing ('BC') in the presence of ω_2T29A that only binds DNA in a sequence-independent manner (26).

Molecular model explaining the role of SC and BC formation

A synergistic interaction between ω_2•*parS* (PC1) and δ_2•DNA (DC), promotes δ_2 relocalization leading to PC2, SC and BC formation, ensuring plasmid pairing. Upon disassembly of the BC, δ_2 polymerization and depolymerization move the plasmids towards the poles leading to accurate segregation (12,26, this work). We propose a sequential, multistep mechanism to position and move the plasmids to cell quarters. In the first step, ω_2 binds cooperatively and with high affinity to *parS* DNA to form a transient left-handed nucleoprotein complex, PC1 (Figure 7A, condition 1), and δ_2 binds *non-parS* DNA forming a transient DC (Figure 7A, conditions 2 and 3) (12,24,44). In step 2, the interaction of δ_2 with PC1 leads to PC2, SC and BC formation (Figure 7A, condition 2); however, when ATP is omitted, the interaction of Apo-δ_2 with PC1 significantly stimulates the accumulation of the long-lived PC2 intermediate (Figure 7A, condition 1). In step 3, ω_2 bound to *parS* interacts with δ_2 bound to *non-parS* to promote dynamic instability of the DC (δ_2•*non-parS* DNA) leading to δ_2 redistribution and co-localization of the PC2 and SC formation (Figure 7A, conditions 1 and 2). In step 4, at low ω_2:δ_2 ratios, the interaction of ω_2 in the PC2 with δ_2 in the SC, facilitates BC formation (Figure 7A, condition 2). In step 5, ω_2, which has dual effects on δ_2 binding to DNA, significantly stabilizes the TC to form 'BC' between two *non-parS* DNA molecules (Figure 7A, condition 3). In step 6, at low ω_2:δ_2 ratios, ω_2 enhances the bulk ATPase activity of δ_2, facilitates the release of ADP-δ_2 from DNA, and stimulates disassembly of the BC or 'BC' (12). Finally, upon disassembly of the pairing complex, the local δ_2 concentration increases in one of the partners leading to a left-handed δ_2•DNA filament onto chromosomal or plasmid DNA (12,44). At high ω_2:δ_2 ratios, ω_2-bound to *parS* DNA inhibits the δ_2 ATPase and chases protein δ_2 off the DNA (re-localization and/or despolymerization) (12). Protein δ_2 polymerization on and de-polymerization from pSM19035 or chromosomal DNA moves the plasmid, as a PC2 cargo, towards the cell poles by an unknown mechanism (Figure 7B). We propose that PC1, DC, PC2, SC and BC formation and δ_2 polymerization–depolymerization, modulated by PC2, are dynamics processes. The molar ω_2:δ_2 ratio and *parS* DNA controls the temporal and spatial partition of pSM19035 before cell division.

SUPPLEMENTARY DATA

Supplementary Data are available at NAR Online.

ACKNOWLEDGEMENTS

We thank K. Takeyasu for advice on AFM analyses and S. Ayora for critical reading of the article. The editorial assistance of the National Institutes of Health Fellows Editorial Board is acknowledged. N.E.S. thanks the JAE-Doc programme and A.V. thanks the fellowship from Comunidad de Madrid (CM), CPI0266/2008.

FUNDING

Ministerio de Ciencias e Innovación (grant nos BFU2009-07167 and CSD2007-00010); CM (grant no. S-2009MAT-1507 to J.C.A.). Funding for open access charge: Spanish Ministry of Science and Innovation.

Conflict of interest statement. None declared.

REFERENCES

1. Ceglowski,P., Boitsov,A., Chai,S. and Alonso,J.C. (1993) Analysis of the stabilization system of pSM19035-derived plasmid pBT233 in *Bacillus subtilis*. *Gene*, **136**, 1–12.
2. Ceglowski,P., Boitsov,A., Karamyan,N., Chai,S. and Alonso,J.C. (1993) Characterization of the effectors required for stable inheritance of *Streptococcus pyogenes* pSM19035-derived plasmids in *Bacillus subtilis*. *Mol. Gen. Genet.*, **241**, 579–585.
3. de la Hoz,A.B., Ayora,S., Sitkiewicz,I., Fernandez,S., Pankiewicz,R., Alonso,J.C. and Ceglowski,P. (2000) Plasmid copy-number control and better-than-random segregation genes of pSM19035 share a common regulator. *Proc. Natl Acad. Sci. USA*, **97**, 728–733.
4. Lioy,V.S., Pratto,F., de la Hoz,A.B., Ayora,S. and Alonso,J.C. (2010) Plasmid pSM19035, a model to study stable maintenance in Firmicutes. *Plasmid*, **64**, 1–17.
5. Rosvoll,T.C., Pedersen,T., Sletvold,H., Johnsen,P.J., Sollid,J.E., Simonsen,G.S., Jensen,L.B., Nielsen,K.M. and Sundsfjord,A. (2010) PCR-based plasmid typing in *Enterococcus faecium* strains reveals widely distributed pRE25-, pRUM-, pIP501- and pHTβ-related replicons associated with glycopeptide resistance and stabilizing toxin-antitoxin systems. *FEMS Immunol. Med. Microbiol.*, **58**, 254–268.
6. Funnell,B.E. (2005) Partition-mediated plasmid pairing. *Plasmid*, **53**, 119–125.
7. Ebersbach,G. and Gerdes,K. (2005) Plasmid segregation mechanisms. *Annu. Rev. Genet.*, **39**, 453–479.
8. Leonard,T.A., Moller-Jensen,J. and Lowe,J. (2005) Towards understanding the molecular basis of bacterial DNA segregation. *Philos. Trans. R. Soc. Lond. B Biol. Sci.*, **360**, 523–535.
9. Hayes,F. and Barilla,D. (2006) The bacterial segrosome: a dynamic nucleoprotein machine for DNA trafficking and segregation. *Nat. Rev. Microbiol.*, **4**, 133–143.
10. Ebersbach,G. and Gerdes,K. (2001) The double *par* locus of virulence factor pB171: DNA segregation is correlated with oscillation of ParA. *Proc. Natl Acad. Sci. USA*, **98**, 15078–15083.
11. Marston,A.L. and Errington,J. (1999) Dynamic movement of the ParA-like Soj protein of *B. subtilis* and its dual role in nucleoid organization and developmental regulation. *Mol. Cell*, **4**, 673–682.
12. Pratto,F., Cicek,A., Weihofen,W.A., Lurz,R., Saenger,W. and Alonso,J.C. (2008) *Streptococcus pyogenes* pSM19035 requires dynamic assembly of ATP-bound ParA and ParB on *parS* DNA during plasmid segregation. *Nucleic Acids Res.*, **36**, 3676–3689.
13. Quisel,J.D., Lin,D.C. and Grossman,A.D. (1999) Control of development by altered localization of a transcription factor in *B. subtilis*. *Mol. Cell*, **4**, 665–672.
14. Hatano,T., Yamaichi,Y. and Niki,H. (2007) Oscillating focus of SopA associated with filamentous structure guides partitioning of F plasmid. *Mol. Microbiol.*, **64**, 1198–1213.
15. Lim,G.E., Derman,A.I. and Pogliano,J. (2005) Bacterial DNA segregation by dynamic SopA polymers. *Proc. Natl Acad. Sci. USA*, **102**, 17658–17663.
16. Ringgaard,S., van Zon,J., Howard,M. and Gerdes,K. (2009) Movement and equipositioning of plasmids by ParA filament disassembly. *Proc. Natl Acad. Sci. USA*, **106**, 19369–19374.
17. Raskin,D.M. and de Boer,P.A. (1999) Rapid pole-to-pole oscillation of a protein required for directing division to the middle of *Escherichia coli*. *Proc. Natl Acad. Sci. USA*, **96**, 4971–4976.
18. Ebersbach,G. and Gerdes,K. (2004) Bacterial mitosis: partitioning protein ParA oscillates in spiral-shaped structures and positions plasmids at mid-cell. *Mol. Microbiol.*, **52**, 385–398.
19. de la Hoz,A.B., Pratto,F., Misselwitz,R., Speck,C., Weihofen,W., Welfle,K., Saenger,W., Welfle,H. and Alonso,J.C. (2004) Recognition of DNA by ω protein from the broad-host range *Streptococcus pyogenes* plasmid pSM19035: analysis of binding to operator DNA with one to four heptad repeats. *Nucleic Acids Res.*, **32**, 3136–3147.
20. Ceglowski,P. and Alonso,J.C. (1994) Gene organization of the *Streptococcus pyogenes* plasmid pDB101: sequence analysis of the *orf* η-*copS* region. *Gene*, **145**, 33–39.
21. Misselwitz,R., de la Hoz,A.B., Ayora,S., Welfle,K., Behlke,J., Murayama,K., Saenger,W., Alonso,J.C. and Welfle,H. (2001) Stability and DNA-binding properties of the ω regulator protein from the broad-host range *Streptococcus pyogenes* plasmid pSM19035. *FEBS Lett.*, **505**, 436–440.
22. Murayama,K., de la Hoz,A.B., Alings,C., Lopez,G., Orth,P., Alonso,J.C. and Saenger,W. (1999) Crystallization and preliminary X-ray diffraction studies of *Streptococcus pyogenes* plasmid pSM19035-encoded ω transcriptional repressor. *Acta Crystallogr. D Biol. Crystallogr.*, **55(Pt 12)**, 2041–2042.
23. Murayama,K., Orth,P., de la Hoz,A.B., Alonso,J.C. and Saenger,W. (2001) Crystal structure of ω transcriptional repressor encoded by *Streptococcus pyogenes* plasmid pSM19035 at 1.5 Å resolution. *J. Mol. Biol.*, **314**, 789–796.
24. Welfle,K., Pratto,F., Misselwitz,R., Behlke,J., Alonso,J.C. and Welfle,H. (2005) Role of the N-terminal region and of β-sheet residue Thr29 on the activity of the ω_2 global regulator from the broad-host range *Streptococcus pyogenes* plasmid pSM19035. *Biol. Chem.*, **386**, 881–894.
25. Weihofen,W.A., Cicek,A., Pratto,F., Alonso,J.C. and Saenger,W. (2006) Structures of ω repressors bound to direct and inverted DNA repeats explain modulation of transcription. *Nucleic Acids Res.*, **34**, 1450–1458.
26. Pratto,F., Suzuki,Y., Takeyasu,K. and Alonso,J.C. (2009) Single-molecule analysis of protein•DNA complexes formed during partition of newly replicated plasmid molecules in *Streptococcus pyogenes*. *J. Biol. Chem.*, **284**, 30298–30306.
27. Lynch,A.S. and Wang,J.C. (1995) SopB protein-mediated silencing of genes linked to the *sopC* locus of *Escherichia coli* F plasmid. *Proc. Natl Acad. Sci. USA*, **92**, 1896–1900.
28. Bouet,J.Y. and Lane,D. (2009) Molecular basis of the supercoil deficit induced by the mini-F plasmid partition complex. *J. Biol. Chem.*, **284**, 165–173.
29. Rodionov,O., Lobocka,M. and Yarmolinsky,M. (1999) Silencing of genes flanking the P1 plasmid centromere. *Science*, **283**, 546–549.
30. Murray,H., Ferreira,H. and Errington,J. (2006) The bacterial chromosome segregation protein Spo0J spreads along DNA from *parS* nucleation sites. *Mol. Microbiol.*, **61**, 1352–1361.
31. Leonard,T.A., Butler,P.J. and Lowe,J. (2005) Bacterial chromosome segregation: structure and DNA binding of the Soj dimer-a conserved biological switch. *EMBO J.*, **24**, 270–282.
32. Hester,C.M. and Lutkenhaus,J. (2007) Soj (ParA) DNA binding is mediated by conserved arginines and is essential for plasmid segregation. *Proc. Natl Acad. Sci. USA*, **104**, 20326–20331.
33. Davey,M.J. and Funnell,B.E. (1994) The P1 plasmid partition protein ParA. A role for ATP in site-specific DNA binding. *J. Biol. Chem.*, **269**, 29908–29913.
34. Davis,M.A., Martin,K.A. and Austin,S.J. (1992) Biochemical activities of the ParA partition protein of the P1 plasmid. *Mol. Microbiol.*, **6**, 1141–1147.
35. Bouet,J.Y., Ah-Seng,Y., Benmeradi,N. and Lane,D. (2007) Polymerization of SopA partition ATPase: regulation by DNA binding and SopB. *Mol. Microbiol.*, **63**, 468–481.
36. Dunham,T.D., Xu,W., Funnell,B.E. and Schumacher,M.A. (2009) Structural basis for ADP-mediated transcriptional regulation by P1 and P7 ParA. *EMBO J.*, **28**, 1792–1802.
37. Barilla,D., Rosenberg,M.F., Nobbmann,U. and Hayes,F. (2005) Bacterial DNA segregation dynamics mediated by the polymerizing protein ParF. *EMBO J.*, **24**, 1453–1464.
38. Ebersbach,G., Ringgaard,S., Moller-Jensen,J., Wang,Q., Sherratt,D.J. and Gerdes,K. (2006) Regular cellular distribution of plasmids by oscillating and filament-forming ParA ATPase of plasmid pB171. *Mol. Microbiol.*, **61**, 1428–1442.

39. Adachi,S., Hori,K. and Hiraga,S. (2006) Subcellular positioning of F plasmid mediated by dynamic localization of SopA and SopB. *J. Mol. Biol.*, **356**, 850–863.
40. Sengupta,M., Nielsen,H.J., Youngren,B. and Austin,S. (2010) P1 plasmid segregation: accurate redistribution by dynamic plasmid pairing and separation. *J. Bacteriol.*, **192**, 1175–1183.
41. Lioy,V.S., Martin,M.T., Camacho,A.G., Lurz,R., Antelmann,H., Hecker,M., Hitchin,E., Ridge,Y., Wells,J.M. and Alonso,J.C. (2006) pSM19035-encoded ζ toxin induces stasis followed by death in a subpopulation of cells. *Microbiology*, **152**, 2365–2379.
42. Riggs,A.D., Bourgeois,S. and Cohn,M. (1970) The Lac repressor-operator interaction. 3. Kinetic studies. *J. Mol. Biol.*, **53**, 401–417.
43. Castaing,J.P., Bouet,J.Y. and Lane,D. (2008) F plasmid partition depends on interaction of SopA with non-specific DNA. *Mol. Microbiol.*, **70**, 1000–1011.
44. Hui,M.P., Galkin,V.E., Yu,X., Stasiak,A.Z., Stasiak,A., Waldor,M.K. and Egelman,E.H. (2010) ParA2, a *Vibrio cholerae* chromosome partitioning protein, forms left-handed helical filaments on DNA. *Proc. Natl Acad. Sci. USA*, **107**, 4590–4595.
45. Ringgaard,S., Lowe,J. and Gerdes,K. (2007) Centromere pairing by a plasmid-encoded type I ParB protein. *J. Biol. Chem.*, **282**, 28216–28225.